

Supramolecular 1D ribbons in complexes between a bicyclic-guanidine derivative and di- or monocarboxylic acids†

Cite this: *CrystEngComm*, 2013, 15, 7321

Vitthal N. Yadav and Carl Henrik Görbitz*

Zwitterionic crystalline complexes between 1,5,7-triazabicyclo[4.4.0]dec-5-ene (**TBD**), a guanidine derivative, and two dicarboxylic acids (DCAs) (oxalic acid, adipic acid) as well as a special monocarboxylic acid (glycolic acid) have been analyzed by single crystal X-ray diffraction methods. In the solid state the carboxylic acid forms a monoanion by readily transferring an acidic proton to a **TBD** base, resulting in formation of strong $^+N-H\cdots O^-$ hydrogen-bonded $R_2^2(8)$ ring motifs, while $O-H\cdots O$ interactions expand the network into infinite one-dimensional supramolecular chains. Numerous $C_{(sp^3)}-H\cdots O$ interactions also contribute in crystal packing, including **TBD** as a weak donor and O atoms of carboxyl groups or co-crystallized water molecules as acceptors. The hydrogen bonding and crystal packing of all three complexes have been compared with the respective guanidine–carboxylate or related complexes reported previously.

Received 30th May 2013,
Accepted 10th July 2013

DOI: 10.1039/c3ce40960k

www.rsc.org/crystengcomm

Introduction

The construction of ordered crystalline networks has been the main focus of supramolecular chemistry in recent decades. To achieve this, molecular recognition through intermolecular non-covalent interactions such as H bonds is the foremost crystal engineering approach.¹ In this area organic acids and bases are appealing building blocks because of their innate and robust H-bonding complex formation capacity, including $N-H\cdots O$, $N\cdots H-O$ and $O-H\cdots O$ interactions.² Unsubstituted guanidine has been extensively incorporated in crystal design and synthesis because of its strong basicity, the unique three-fold structural symmetry of the guanidinium cation, and the ability to form charge-assisted $^+N-H\cdots O^-$ hydrogen bonds with carboxylate, phosphonate, sulphonate and nitro groups *etc.* that often results in formation of the symmetrical $R_2^2(8)$ H-bonding motif (Fig. 1a)³ in diverse 2D or 3D networks.⁴

The guanidine derivative **TBD** (Fig. 1b) is a rigid and versatile building block that has been widely used as a ligand in co-ordination chemistry⁵ and often serves as a base⁶ or a catalyst⁷ in organic synthesis. Use of **TBD** in supramolecular chemistry, on the other hand, has been poorly investigated, and only few crystal structures have been reported.^{3f,7,8} Recently, we have demonstrated that the **TBD** cation with only two donor sites is in fact a structurally interesting building block when combined with a partner bipyridine

dicarboxylate.⁹ Subsequently we have illustrated different structural properties of **TBD**–carboxylates *via* several 2 : 1 (**TBD** : DCA) crystalline complexes which form various H-bonded motifs. In these complexes the *anti* lone pairs of carboxylate O atoms often interact with co-crystallized water molecules by H bonding.¹⁰ These waters of hydration lead into well organized water clusters, 1D tapes or open channels rather than the hexagonal networks or densely packed structures obtained in native guanidine complexes.^{4,9,11}

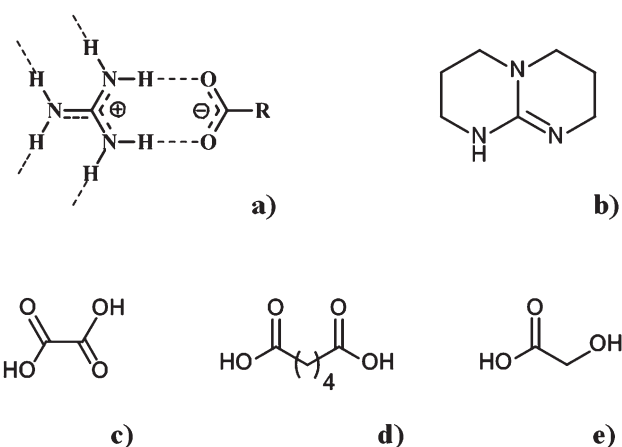


Fig. 1 a) A hydrogen bonded guanidinium–carboxylate recognition adduct forming $R_2^2(8)$ motif. b) **TBD** a base and c) oxalic acid d) adipic acid e) glycolic acid used in complexes.

Department of Chemistry, University of Oslo, Post box 1033, Blindern, Oslo – 0315, Norway. E-mail: c.h.gorbitz@kjemi.uio.no; Fax: +47 228 55 441

† CCDC 905593–905595. For crystallographic data in CIF or other electronic format see DOI: 10.1039/c3ce40960k



In contrast to the earlier 2 : 1 complexes, the present work is focusing on unusual solid-state structures formed by **TBD** ($pK_a = 14.47$)¹² with oxalic acid (**OxT**, Fig. 1c, $pK_{a1} = 1.27$; $pK_{a2} = 4.27$), adipic acid (**AdT**, Fig. 1d, $pK_{a1} = 4.41$; $pK_{a2} = 5.41$) and glycolic acid (**GiT**, Fig. 1e, $pK_a = 3.83$).¹³

Experimental

Materials and general process for crystal preparation

TBD, oxalic acid, adipic acid and glycolic acid were purchased from Sigma-Aldrich and used as received. X-ray quality single crystals were obtained by dissolving **TBD** (2 mmol) and the corresponding carboxylic acid (1 mmol) in demineralized water (2 ml). The mixture was stirred for 10 minutes at ambient temperature and kept stationary to evaporate the solvent slowly over 3–4 weeks. ^1H -NMR and ^{13}C -NMR data for the obtained complexes were recorded at RT using a Bruker DPX300MHz spectrometer. Melting point (mp) measurements were performed using Stuart SMP10 equipment.

TBD:hydrogen oxalate (OxT)

mp 138–140 °C.

^1H -NMR, 300 MHz, (DMSO- d_6) δ 10.38 (s, 2H), 3.27–3.23 (t, 8H), 3.15–3.11 (t, 8H), 1.90–1.82 (m, 8H).

^{13}C -NMR, 300 MHz, (DMSO- d_6) δ , 173.09 (COO), 151.92 (CN₃), 46.94 (CH₂), 38.06 (CH₂), 21.39 (CH₂).

TBD:hydrogen adipate (AdT)

mp 238–240 °C.

^1H -NMR 300 MHz, (DMSO- d_6 + D₂O) δ , 3.23–3.19 (t, 8H), 3.13–3.09 (t, 8H), 1.94–1.89 (m, 4H), 1.87–1.79 (m, 8H), 1.39–1.34 (m, 4H).

^{13}C -NMR 300 MHz, (DMSO- d_6 + D₂O) δ , 180.48 (COO), 151.69 (CN₃), 46.88 (CH₂), 38.60 (CH₂), 37.88 (CH₂), 26.98 (CH₂), 21.11 (CH₂).

TBD:glycolate monohydrate (GiT)

mp 88–90 °C.

^1H -NMR, 300 MHz (DMSO- d_6) δ , 9.93 (s, 1H), 3.51 (s, 2H), 3.28–3.24 (t, 4H), 3.17–3.13 (t, 4H), 1.91–1.83 (m, 4H).

^{13}C -NMR 300 MHz (DMSO- d_6) δ , 177.29 (COO), 152.04 (CN₃), 62.24 (CH₂), 46.96 (CH₂), 38.05 (CH₂), 21.29 (CH₂).

X-ray structure determination

X-ray intensity data measurements of **OxT**, **AdT** and **GiT** crystalline complexes were carried out on a Bruker SMART APEX II CCD diffractometer with graphite-monochromatized (Mo $\text{K}\alpha = 0.71073$ Å) radiation at low temperature (105 K) controlled by an Oxford Cryostream low-temperature device. Data were collected with ω scan width 0.5° at three different settings of φ (0°, 90° and 180°) with the detector fixed at $2\theta = -30$ °. Data integration/reduction and absorption was carried out by SAINT and SADABS, respectively, refinement by SHELXTL.¹⁴ In these complexes all the H–C and the H–N hydrogen atoms were constrained to theoretical positions. The carboxylic (O–H) H-atoms of **OxT** and **AdT**, and an alcoholic (O–H) and H-atoms of a co-crystallized water molecule in **GiT** were added from the experimental Fourier difference electron density diffraction map. The **GiT** water molecule is observed to be disordered over three sites (O1W, O2W and O3W) with refined occupancies 0.900(7), 0.056(7) and 0.042(4), respectively. The O–H bond lengths of the water molecule were subject to SHELX restraints (see CIF file). The program Mercury¹⁵ was used to generate the molecular and packing illustrations of all the complexes. Crystal data are summarized in Table 1.

Table 1 Crystallographic data

Crystal	OxT	AdT	GiT
Unit formula	C ₉ H ₁₅ N ₃ O ₄	C ₁₃ H ₂₃ N ₃ O ₄	C ₉ H ₁₇ N ₃ O ₃ H ₂ O
Crystal size/mm	0.90 × 0.30 × 0.10	0.40 × 0.20 × 0.15	0.55 × 0.30 × 0.10
Unit weight	229.23	285.37	233.25
Crystal system	Orthorhombic	Monoclinic	Triclinic
Space group	P ₂ 12 ₁ 2 ₁	P2 ₁ /c	P ₁
<i>a</i> /Å	7.8795(16)	7.014(3)	7.1832(7)
<i>b</i> /Å	9.760(2)	12.065(5)	8.9257(9)
<i>c</i> /Å	13.612(3)	17.179(7)	9.8008(10)
$\alpha/^\circ$	90	90	71.298(1)
$\beta/^\circ$	90	90.118(6)	75.374(1)
$\gamma/^\circ$	90	90	81.203(1)
<i>V</i> /Å ³	1046.8(4)	1453(10)	574.13(10)
<i>Z</i>	4	4	2
Density/g cm ⁻³	1.455	1.304	1.349
Absorption coefficient/mm ⁻¹	0.12	0.10	0.11
θ range for data collection/°	2.6–28.9	2.1–28.5	2.3–28.7
Reflections	Collected Independent Observed	9443 1592 1536	10 766 3687 2527
<i>R</i> _{int}	0.019	0.061	0.011
wR(F ²)	0.0710	0.133	0.094
<i>R</i> [F ² > 2σ(F ²)]	0.0278	0.053	0.034



Results and discussion

Complex **OxT**

The anhydrous orthorhombic crystals of **OxT** contain a hydrogen oxalate anion and a **TBD** cation in the asymmetric unit (Fig. 2a). The O1 and O2 atoms of the oxalate are H-bonded to **TBD** so as to form a symmetrical $R_2^2(8)$ ring motif as shown in Fig. 1a. The carboxyl H-atom (H4O) of the hydrogen oxalate is donated to an *anti* lone pair of O1 (for details of H-bond data see Table 2). This strong carboxyl–carboxylate ($\text{COOH}\cdots\text{OOC}$) interaction leads to formation of an infinite 1D chain of hydrogen oxalate along the *a*-axis that is decorated by **TBD** cations (Fig. 2b). The resulting ribbons are densely stacked in a herringbone-like array as shown in Fig. 2c, where the polar hydrogen oxalate chain at the core appears to be encapsulated by the neighboring hydrophobic **TBD** moieties.

Unlike the three-dimensionally H-bonded structure of regular guanidinium–hydrogen oxalate hydrate^{4a} (refcode GUHOXM, Cambridge Structure Database,¹⁶ CSD v5.34, Nov. 2012), the hydrogen oxalate in **OxT** is non-planar and exists in a twisted conformation [torsion angle O1–C8–C9–O3 = $-54.13(15)^\circ$] to facilitate formation of the 1D chain. Such an adapted orientation of hydrogen oxalate in **OxT** clearly deviates from the theoretical 90° torsion angle of oxalate.¹⁷ Thus, the crystal structure of **OxT** demonstrates that by reducing the H-bond complexity of the guanidinium ion, the molecular assembly can be directed towards a less complicated 1D supramolecular structure.

Complex **AdT**

The asymmetric unit of **AdT** (Fig. 3a) and the formation of one-dimensional ribbons driven by carboxyl–carboxylate H bonding (Fig. 3b) are closely reminiscent of the observations made for **OxT** (Fig. 2a and 2b). However, there are two obvious differences between these two structures: first the carboxylate groups of adipic acid are not directly connected as for oxalic acid, but separated by the $-(\text{CH}_2)_4-$ linker, and second the 1D ribbons of **AdT** are planar and aligned two-dimensionally in the crystallographic *bc*-plane to form an interlocked sheet-like topology (Fig. 3b), whereas **OxT** shows a non-planar herring-

Table 2 Selected hydrogen-bond distances (Å) and angles ($^\circ$)^a

D–H \cdots A	D–H	H \cdots A	D \cdots A	$\angle(\text{D–H}\cdots\text{A})$
Crystal OxT				
N1–H1 \cdots O1	0.86	1.98	2.839(14)	179
N3–H3 \cdots O2 ⁱ	0.86	1.94	2.817(13)	174
O4–H4O \cdots O1 ⁱ	0.90(2)	1.65(2)	2.549(13)	172(18)
Crystal AdT				
N1–H1 \cdots O1 ⁱⁱ	0.88	1.92	2.796(2)	179
N3–H3 \cdots O2 ⁱⁱ	0.88	1.85	2.723(2)	173
O4–H4 \cdots O2 ⁱⁱⁱ	0.99(3)	1.56(3)	2.536(2)	170(3)
Crystal GIT				
N1–H1 \cdots O1	0.88	1.98	2.855(11)	176
N3–H3 \cdots O2	0.88	1.89	2.772(11)	176
O3–H3O \cdots O1 ^{iv}	0.85(17)	1.96(17)	2.741(11)	152(14)
O1W–H11W \cdots O2	0.87(2)	1.93(2)	2.802(12)	176(19)
O1W–H12W \cdots O3 ^v	0.83(2)	2.06(2)	2.887(14)	174(2)

^a Symmetry codes i) $x - 1/2, 1/2 - y, 1 - z$; ii) $-x + 1, -y + 1, -z + 1$; iii) $x, -y + 3/2, z + 1/2$; iv) $-x, 1 - y, 2 - z$; v) $-x, -y, 2 - z$.

bone-like pattern. The sheets in **AdT** are stacked within the $\pi\cdots\pi$ interplanar distance range $\sim 3.1\text{--}3.7$ Å [for $_{(\text{N}1\text{--N}2\text{--N}3)}\text{TBD}\cdots\text{TBD}'_{(\text{N}1\text{--N}2\text{--N}3)}$ and $(\text{COO}^-\cdots\text{COO}^-)$] and within the van der Waals space of $2.287\text{--}2.394$ Å for adipate/TBD $_{(\text{sp}3)}$ –H \cdots H–C $_{(\text{sp}3)}$ –adipate (Fig. S1, ESI†).

The crystallization experiment between the adipic acid and **TBD** was set up to obtain a 2 : 1 crystalline complex containing two **TBD** cations and a dianion of adipic acid. In fact, the resulting **AdT** crystal contains a monoanion rather than a dianion. To facilitate a second deprotonation step by breaking the strong carboxyl–carboxylate interaction, three additional crystallization experiments with increased **TBD** concentrations (adipic acid : **TBD** ratios 1 : 3, 1 : 4 and 1 : 5) and one controlled experiment with 1 : 1 ratio were carried out. The 1 : 1 mixture instantaneously afforded the familiar **AdT** type of crystal, whilst other mixtures did not yield crystals. This apparently confirms that the 1 : 1 ratio of adipic acid and **TBD** is the thermodynamically favorable composition for crystal formation.

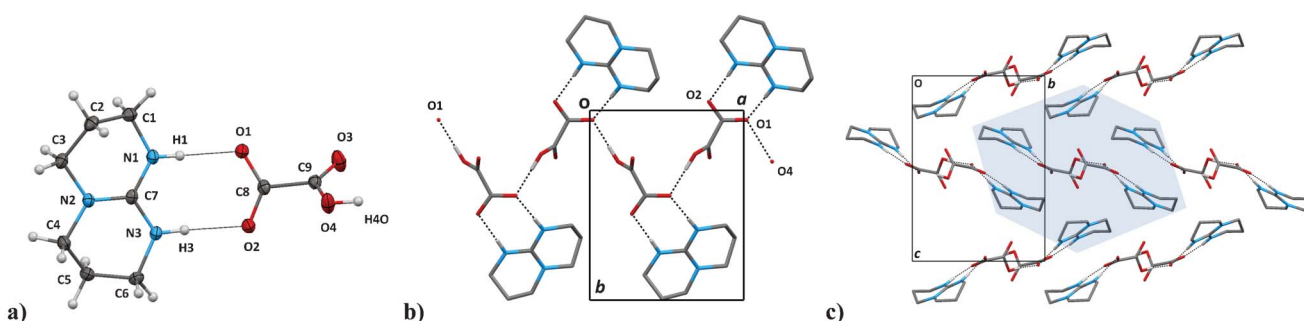


Fig. 2 a) The asymmetric unit of **OxT** with atomic label scheme. Displacement ellipsoids are shown at the 50% probability level. b) Capped stick representation of one-dimensional hydrogen bonded molecular ribbon in **OxT** viewed down the crystallographic *c*-axis. Hydrogen atoms not involved in hydrogen bonds have been omitted for clarity. c) Three-dimensional herringbone pattern of 1D ribbons in the crystal packing of **OxT** viewed along the *a*-axis. At the core, the highlighted light-blue shade represents the encapsulation of polar hydrogen–oxalate chain by hydrophobic **TBD** molecules.



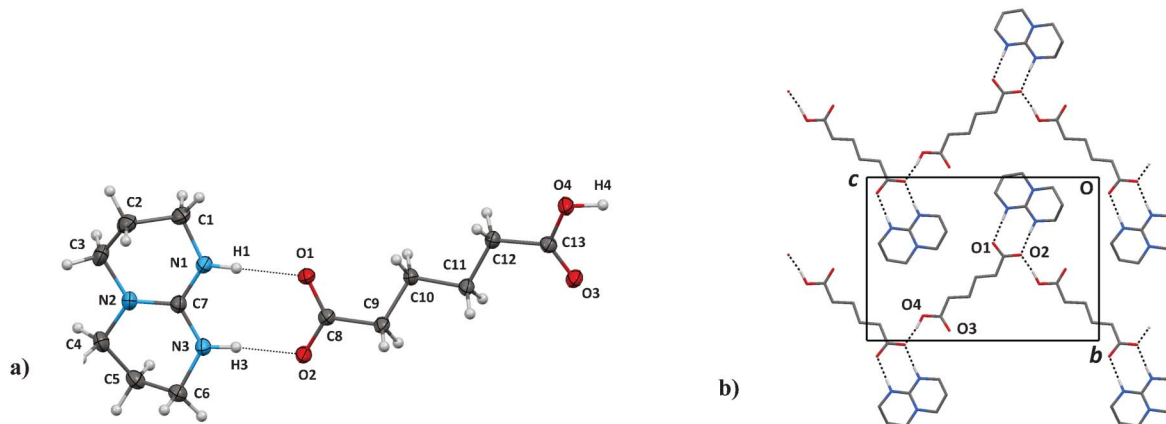


Fig. 3 a) The asymmetric unit of crystal **AdT** with atom label scheme. Displacement ellipsoids are shown at the 50% probability level. b) The 1D infinite chains in **AdT** running along the crystallographic *c*-axis. These chains are interlocked in a zigzag pattern which forms a layer parallel to plane-*bc*. The non-hydrogen bonded hydrogen atoms have been omitted for clarity.

In theory, a dicarboxylic acid should form a dianion upon proton exchange with a base, though in reality the structural characteristics of the acid and base involved may also promote formation of monoanions. This is clear from a survey of dicarboxylic acids in the CSD, where mono- and dianions of oxalic acid are equally common (~190 structures each). The distribution between mono- and dianion for succinic acid with a $-\text{CH}_2\text{CH}_2-$ linker ($\text{Succ}^- = 48$; $\text{Succ}^{2-} = 65$) and adipic acid ($\text{Adp}^- = 13$; $\text{Adp}^{2-} = 34$), reveals a trend: when the aliphatic link between the two carboxylic groups is extended, the ratio of mono/dianion decreases.

Complex GIT

The asymmetric unit of the **GIT** complex is composed of the glycolate anion, **TBD** and a water molecule (Fig. 4a). The **TBD** and glycolate ions are H bonded by two $^+\text{N-H}\cdots\text{O}^-$ interactions forming a $\text{R}_2^2(8)$ motif. An **TBD**-glycolate complex is interacting with another **TBD**-glycolate through glycolate $\text{O-H}\cdots\text{O}$ carboxylate interactions and generating a tetramer through the new $\text{R}_2^2(10)$ ring motif, (Fig. 4b). Co-crystallized water molecules serve as links between tetramers through formation of a third hydrogen bonded ring motif, $\text{R}_4^4(14)$, thus producing a supramolecular ribbon along the *b*-axis (Fig. 4b). The compact

and staggered spatial arrangement of ribbons in **AdT** is significantly influenced by the weak interactions such as $\text{N}_1\cdots\text{H}_{62}\text{C}_6$ (2.67 Å) and $\text{C-H}\cdots\text{O}$ (see Table 3).

There is no crystal structure involving native guanidine and glycolic acid in the CSD, but a close structural analogue, the guanidinium-bicarbonate, is reported (refcode: DUMPW).¹⁸ This bicarbonate is a methylene group shorter than the glycolate, but it forms a very similar H-bonded tetramer. As the bicarbonate salt is devoid of water molecules, the tetramers are, however, not linked into chains but generate a compact 3D network (see ESI,† Fig. S2).

C-H \cdots O interactions and crystal packing

Although the C-H \cdots O hydrogen bond is a weak non-covalent interaction, in molecular self-assembly its role is proficient enough to direct the 3D aggregations. This interaction is formed between C and O atoms within a distance range of 3.0–4.0 Å.¹⁹ In the present study the $\text{N-H}\cdots\text{O}$ and $\text{O-H}\cdots\text{O}$ hydrogen bonds are electrostatic and directive in binary crystalline complex formation. The role of the aliphatic skeleton of **TBD** and its contribution to the crystal packing is more variable due to the conformational flexibility of the fused ring system and the multiple and nondirective weak C-H

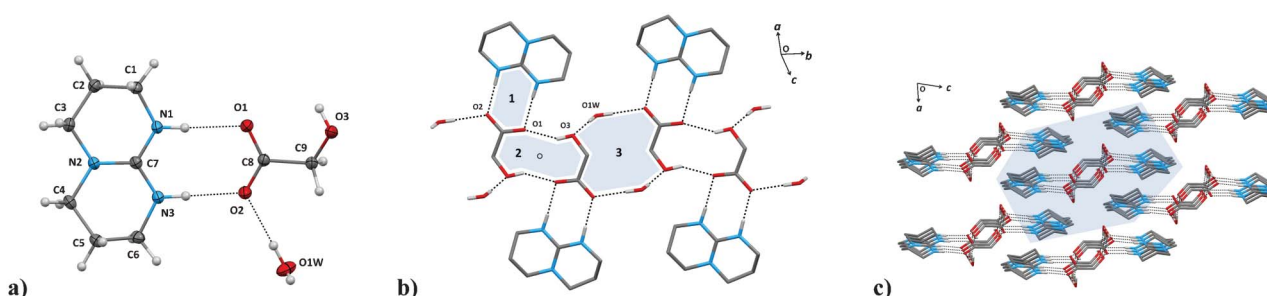


Fig. 4 a) The asymmetric unit of **GIT**. Displacement ellipsoids are shown at the 50% probability level. b) One-dimensional infinite molecular ribbon in **GIT**. Three hydrogen bonded ring motifs, 1, $\text{R}_2^2(8)$; 2, $\text{R}_2^2(10)$ and 3, $\text{R}_4^4(14)$ have been highlighted by light-blue shades. A small circle represents the inversion centre of symmetry. c) The crystal packing of one-dimensional ribbons viewed along the *b*-axis. Light-blue shade represents the hydrophobic surroundings of adipate:water chain. Hydrogen atoms except H bonded have been omitted for clarity in b) and c).

Table 3 C-H···O interactions with distances (Å) and angles (°)

Complex	C-H···O	C-H···O	C···O	∠(C-H···O)
OxT	C3-H31···O4	2.54	3.258(2)	128.5
	C6-H61···O3	2.61	3.590(2)	167.0
AdT	C2-H22···O3	2.54	3.485(4)	158.9
	C6-H62···O4	2.59	3.394(4)	137.8
GiT	C5-H51···O1	2.45	3.237(2)	135.3

donor implications. In the **OxT**, **AdT** and **GiT** structures there is a variety of C-H···O interactions between the **TBD** methylene H atoms and strong H-bond accepting O atoms in either the carboxyl groups (see Fig. 5a and 5b) or water (Fig. 5c), which are greatly involved in creating a densely packed crystalline network. The carboxyl group in **OxT** coordinates with two **TBD** from different layers and forms H-O···H-C₃ and >C=O···H-C₆ contacts, (bond lengths and angles are summarized in Table 3), where both the **TBD** orient perpendicularly to the carboxyl plane to avoid steric conflict (Fig. 5a). By contrast, in **AdT** the carboxyl group of the planar and layered hydrogen adipate is aligned parallel to the plane of **TBD**, interacting with H-C₂ and H-C₆ (Fig. 5b). Exceptionally the C-H···O interaction in **GiT** involves an additional solvated water molecule as acceptor rather than a carboxylate which is fully engaged in strong H bonding with the **TBD** and water (Fig. 5c).

Conclusion

Here we have pursued a crystalline complex formation approach based on the R₂²(8) synthon formed by dicarboxylic

acids and a **TBD** base. This strategy implies controlling the capacity of a potential multiple H-atom donor such as native guanidinium cation. This restrictive path can generate ordered and relatively less complicated lower order crystalline molecular networks (e.g. **OxT** and **GiT**). Complexes building an infinite H-bonded network of 1D-chains or tapes, are of interest for materials such as gelators.²⁰ Hence this method may provide a model for further materials preparation. **TBD** and its weak aliphatic C-H co-ordination should offer insight into the structurally and biologically relevant interactions of similar groups of molecules.

Notes and references

- (a) G. R. Desiraju, *Crystal Engineering: The Design of Organic Solids*, Elsevier, Amsterdam, 1989; (b) G. R. Desiraju, *Angew. Chem., Int. Ed. Engl.*, 1995, **34**, 2311–2327; (c) C. B. Aakeroy and K. R. Seddon, *Chem. Soc. Rev.*, 1993, **22**, 397–407.
- (a) G. R. Desiraju, *Acc. Chem. Res.*, 2002, **35**, 565–573; (b) O. Félix, M. W. Hosseini, A. De Cian and J. Fischer, *Angew. Chem., Int. Ed. Engl.*, 1997, **36**, 102–104; (c) A. Mukherjee and G. R. Desiraju, *Chem. Commun.*, 2011, **47**, 4090–4092; (d) M. Du, Z.-H. Zhang and X.-J. Zhao, *Cryst. Growth Des.*, 2005, **5**, 1199–1208; (e) H. P. Jones, R. J. Davey and B. G. Cox, *J. Phys. Chem. B*, 2005, **109**, 5273–5278; (f) J. F. Remenar, S. L. Morissette, M. L. Peterson, B. Moulton, J. M. MacPhee, H. R. Guzmán and Ö. Almarsson, *J. Am. Chem. Soc.*, 2003, **125**, 8456–8457; (g) S.-p. Chen, L.-l. Pan, Y.-x. Yuan, X.-x. Shi and L.-j. Yuan, *Cryst. Growth Des.*, 2009, **9**, 2668–2673; (h) D. R. Trivedi and P. Dastidar, *Cryst. Growth Des.*, 2006, **6**, 1022–1026; (i) K. Kinbara, Y. Hashimoto, M. Sukegawa, H. Nohira and K. Saigo, *J. Am. Chem. Soc.*, 1996, **118**, 3441–3449; (j) J. C. MacDonald, P. C. Dorrestein and M. M. Pilley, *Cryst. Growth Des.*, 2001, **1**, 29–38.
- (a) M. C. Etter, *Acc. Chem. Res.*, 1990, **23**, 120–126; (b) E. D. Raczyńska, M. K. Cyrański, M. Gutowski, J. Rak, J.-F. Gal, P.-C. Maria, M. Darowska and K. Duczmal, *J. Phys. Org. Chem.*, 2003, **16**, 91–106; (c) J. Han, C.-W. Yau, C.-K. Lam and T. C. W. Mak, *J. Am. Chem. Soc.*, 2008, **130**, 10315–10326; (d) W.-Z. Xu, J. Sun, Z.-T. Huang and Q.-Y. Zheng, *Chem. Commun.*, 2009, 171–173; (e) A. C. Soegiarto, A. Comotti and M. D. Ward, *J. Am. Chem. Soc.*, 2010, **132**, 14603–14616; (f) K. Latham, J. E. Downs, C. J. Rix and J. M. White, *J. Mol. Struct.*, 2011, **987**, 74–85.
- (a) J. Adams, *Acta Crystallogr., Sect. B: Struct. Crystallogr. Cryst. Chem.*, 1978, **34**, 1218–1220; (b) V. Videnova-Adrabinska, E. Obara and T. Lis, *New J. Chem.*, 2007, **31**, 287–295; (c) G. Smith, U. D. Wermuth, D. J. Young and P. C. Healy, *Acta Crystallogr., Sect. E: Struct. Rep. Online*, 2007, **63**, o556–o557; (d) G. Smith and U. D. Wermuth, *Acta Crystallogr., Sect. C: Cryst. Struct. Commun.*, 2010, **66**, o575–o580.
- (a) S. H. Oakley, D. B. Soria, M. P. Coles and P. B. Hitchcock, *Dalton Trans.*, 2004, 537–546; (b) U. Wild, P. Roquette, E. Kaifer, J. Mautz, O. Hübner, H. Wadebold and H.-J. Himmel, *Eur. J. Inorg. Chem.*, 2008, **2008**, 1248–1257; (c) M. P. Coles, *Chem. Commun.*, 2009, 3659–3676.

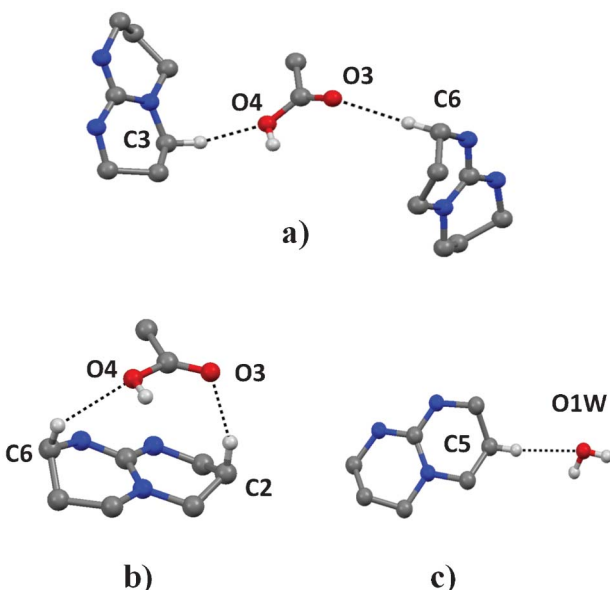


Fig. 5 C-H···O interactions formed by **TBD** with a) carboxyl in **OxT**, b) and **AdT**, and c) with water in **GiT**.



6 (a) D. Simoni, M. Rossi, R. Rondanin, A. Mazzali, R. Baruchello, C. Malagutti, M. Roberti and F. P. Invidiata, *Org. Lett.*, 2000, **2**, 3765–3768; (b) D. J. Phillips and A. E. Graham, *Synlett*, 2010, **769**, 773; (c) R. C. Pratt, B. G. G. Lohmeijer, D. A. Long, R. M. Waymouth and J. L. Hedrick, *J. Am. Chem. Soc.*, 2006, **128**, 4556–4557.

7 C. D. N. Gomes, O. Jacquet, C. Villiers, P. Thuéry, M. Ephritikhine and T. Cantat, *Angew. Chem., Int. Ed.*, 2012, **51**, 187–190.

8 (a) I. Binkowska, A. Jarczewski, A. Katrusiak, G. Wojciechowski and B. Brzezinski, *J. Mol. Struct.*, 2001, **597**, 101–107; (b) A. Huczyński, M. Ratajczak-Sitarz, A. Katrusiak and B. Brzezinski, *J. Mol. Struct.*, 2008, **888**, 84–91.

9 V. N. Yadav and C. H. Görbitz, *CrystEngComm*, 2013, **15**, 439–442.

10 V. N. Yadav and C. H. Görbitz, *Cryst. Growth Des.*, 2013, **13**, 2174–2180.

11 T. C. W. Mak and F. Xue, *J. Am. Chem. Soc.*, 2000, **122**, 9860–9861.

12 pK_a , Calculated using Advanced Chemistry Development (ACD/Labs) Software V11.02 (©1994–2013 ACD/Labs).

13 H. C. Brown, D. H. McDaniel and O. Häfdinger, *Determination of Organic Structures by Physical Methods*, ed. E. A. Braude and F. C. Nachod, Academic Press, New York, 1955.

14 (a) Bruker APEX2, SAINT-Plus and SADABS, Bruker AXS Inc., Madison, Wisconsin, USA, 2007; (b) G. Sheldrick, *Acta Crystallogr., Sect. A: Found. Crystallogr.*, 2007, **64**, 112–122.

15 C. F. Macrae, I. J. Bruno, J. A. Chisholm, P. R. Edgington, P. McCabe, E. Pidcock, L. Rodriguez-Monge, R. Taylor, J. van de Streek and P. A. Wood, *J. Appl. Crystallogr.*, 2008, **41**, 466–470.

16 F. Allen, *Acta Crystallogr., Sect. B: Struct. Sci.*, 2002, **58**, 380–388.

17 D. Y. Naumov, E. V. Boldyreva, N. V. Podberezskaya and J. A. K. Howard, *Solid State Ionics*, 1997, **101–103**, 1315–1320.

18 D. A. Baldwin, L. Denner, T. J. Egan and A. J. Markwell, *Acta Crystallogr., Sect. C: Cryst. Struct. Commun.*, 1986, **42**, 1197–1199.

19 (a) G. R. Desiraju and T. Steiner, *The Weak Hydrogen Bond In Structural Chemistry and Biology*, Oxford University Press, Oxford, 1999; (b) G. R. Desiraju, *Acc. Chem. Res.*, 1996, **29**, 441–449; (c) T. Steiner, *Crystallogr. Rev.*, 2003, **9**, 177–228.

20 R. Luboradzki, O. Gronwald, M. Ikeda, S. Shinkai and D. N. Reinhoudt, *Tetrahedron*, 2000, **56**, 9595–9599.

